

Use of a Large-Scale, Spectral Wave Generation Model to Define Input into Nearshore Wave Transformation Model

Brian A. Caufield and Kirk F. Bosma

Woods Hole Group
81 Technology Park Drive
East Falmouth, Massachusetts, USA 02536
508-540-8080

1. INTRODUCTION

Woods Hole Group, Inc. worked with the US Army Corps of Engineers (USACE) on a Section 111 Project at Saco River and Camp Ellis Beach in southeastern Maine. This project focuses on the erosion adjacent to a federally constructed and maintained navigational structure at the mouth of the Saco River. This area has experienced erosion [7,12] since the construction and multiple adjustments to the navigational structures have been made. The Section 111 study involved both an extensive field data collection program and a numerical wave-modeling program. The first numerical wave model used was a model to evaluate the offshore, deep-water wave environment. This generation-scale model was used to define spectral input into the more detailed, shallow-water wave transformation model.

Numerical models are only as good as the quality of the data used to specify forcing conditions, calibrate and verify the model. Data used to calibrate the transformation wave model were based on up-to-date, accurate measurements at two locations within Saco Bay. Data specified at the boundary condition, however, had to be developed based on currently maintained buoys and/or historical hindcast data, which have both temporal and directional limitations. The Wave Information System (WIS) hindcast data contains directional spectra, but not for the same time period when the interior wave data were collected (March-May 2003). A correlation between historical directional spectra and wave height observations at the buoy locations would be required in order to utilize the WIS data for calibration time periods. Therefore, the WIS data has limited use for specifying the boundary condition to calibrate the regional wave model. Likewise, although the buoys in the vicinity of the Saco Bay region are currently measuring data, the data are non-directional. Therefore, buoy data also have limited use as a boundary condition to calibrate the regional wave model since the direction of these wave fields is unknown. Additionally, the location of the existing offshore buoys and hindcast data are spatially limited (e.g., do not correspond directly to the offshore boundary of the wave model). To improve upon these limitations, regional wind fields and an offshore, spectral, wave generation model was applied for the time period of the field data collection program (March-May

2003) to provide wave-forcing information directly at the boundary of the transformation wave model.

This paper discusses the numerical model used in the generation-scale numerical wave model, the calibration and verification procedure used in this task and the process by which this model was used to provide input into the transformation model.

2. BACKGROUND

Saco River/Camp Ellis Beach is located in southeastern Maine (Figure 1) on the Atlantic Ocean. The nearshore zone has a complex bathymetry with several offshore islands and submerged features. This complex nearshore bathymetry required the use of state-of-the-art numerical wave models for engineering design. As part of the Section 111 study, Woods Hole Group deployed two bottom-mounted Acoustic Doppler Current Profilers (ADCP). One ADCP was placed offshore of two islands in about 10 m water depth. The second ADCP was located inshore of these two islands in approximately 4 m water depth. The data from these instruments were to be used during the calibration and verification task of the transformation and nearshore wave modeling programs of the project. A more detailed explanation of the physical setting and a detailed project overview can be found in Bosma and Caufield [1].

The goal of the offshore modeling for Camp Ellis Beach was to simulate wave growth, dissipation and propagation in deep-water for use as input into the transformation wave modeling task. The transformation wave modeling effort would transform the wave energy from deep water to shallow water. To accomplish this offshore modeling goal, Woods Hole Group applied the spectral wave model, WAVAD [11]. The model used input wind fields as the primary generating force for deep-water waves. The model output included wave spectra at equi-spaced points within the area of interest. It was necessary to utilize a spectral wave model because the transformation task used a spectral model (STWAVE).

The modeled wave spectra represented the distribution of wave energy with respect to frequency and direction, in discretized frequency and direction bands. Propagation effects and source/sink mechanisms were computed in terms

of variations in energy levels in each of these frequency-direction elements. All wave parameters such as significant wave height, frequency of the spectral peak, and mean wave direction were computed from these discrete elements.

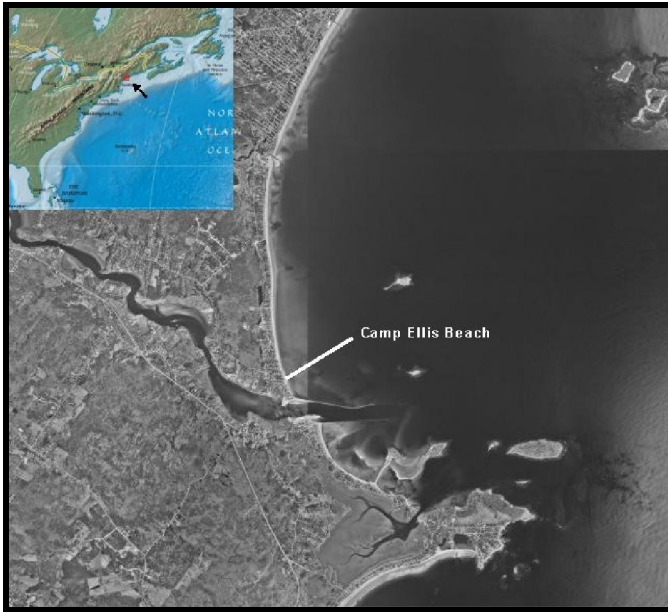


Fig. 1. Project location.

3. WAVE MODEL

The physics embodied in WAVAD represent an f^4 equilibrium range formulation, as supported by field experiments [3, 5, 6 and 13], and is consistent with energy conservation in the equilibrium range, as calculated from the complete or reduced Boltzmann integrals. The fetch-growth characteristics of the model are similar to the JONSWAP relationships (i.e. wave energy increased linearly with fetch) and the duration-growth characteristics are roughly similar to those of Resio [8] and the Navy's Spectral Ocean Wave Model (SOWM).

In a coordinate system moving with the group velocity of the spectral peak, the governing equation for the evolution of the wave spectrum can be approximated as:

$$\frac{DE(f)}{Dt} = S_1(f) + S_2(f) + S_3(f) + S_4(f) + S_5(f)$$

where $S_i(f)$ represents a separate source term:

- $S_1(f)$ = shoaling,
- $S_2(f)$ = refraction,
- $S_3(f)$ = wind effects,
- $S_4(f)$ = wave-wave interactions and
- $S_5(f)$ = bottom interaction effects

The WAVAD model represents each of these processes using methodologies developed from theory and experiments.

The WAVAD model propagates each frequency-direction element independently using an upstream differencing method, which offers advantages for stability, execution time and set-up simplicity. In a latitude-longitude grid as used in this model, propagation along meridians (or components of propagation along meridians) is the equivalent of propagation along great circles. Consequently, there is no curvature away from a straight-line propagation along these axes; however, divergence/convergence effects are incorporated for meridional propagation. For propagation along latitudes (parallels), there is no divergence/convergence; however, angular curvature must be considered. When a "square grid" is set up, curvature and divergence effects become zero.

Proper simulation of the physics of energy transfer into and out of each element in the directional spectrum is essential for accurate wave modeling. WAVAD uses the following simulated sources and sinks of energy:

- Energy transfer from the atmosphere (winds) to the wave field,
- Energy transfers among wave components (wave-wave interactions),
- Energy losses due to wave breaking,
- Bottom friction

Each of these sources and sinks is discussed below.

The total energy input into the wave spectra from the wind is given by:

$$\frac{\partial E_o}{\partial t} = \frac{Ru^3}{g}$$

Where R is a dimensionless constant, g is gravity, E_o is the one-dimensional wave spectrum, and u is the wind speed. This equation is consistent with the concept that, at oceanic scales, the coefficient of drag is independent of the wave height; therefore, the total energy transfer rate from the atmosphere to the water is independent of wave height.

Theoretical considerations dictate that certain geometric constraints on wave-wave interactions effectively force the wave spectrum toward a characteristic similarity form. As a result the energy balance between nonlinear fluxes and wind inputs leads to an equilibrium range of the f^4 type [9,10].

The WAVAD model assumes that wave breaking removes all energy that is transferred into frequencies above some threshold frequency.

Bottom friction follows a quadratic formulation, which, following Collins [2], leads to a rate of energy loss given by:

$$\frac{\partial E(f, \theta)}{\partial t} = -\frac{E(f, \theta) C_f g k^2}{2\pi \omega^2 \cosh(kh)} \langle u \rangle$$

where

$$u = \left[\int \frac{E(f) g^2 k^2}{\omega^2 \cosh^2(kh)} df \right]^{1/2}$$

And k is the wave number, h is the water depth, $E(f, \theta)$ is the 3-D spectrum, ω is the angular frequency, and C_f is the bottom friction coefficient.

4. MODEL INPUTS

4.1. Model Grid

Solutions in the offshore wave model were computed on a rectangular grid, which had equal sized x and y increments. The axes of the grid were aligned with latitude-longitude lines. Any point in the grid can be denoted by (I, J) coordinates, where I referenced the columns and J referenced the rows. Grid point $(I=1, J=1)$ is in the lower left corner of the grid.

For simulations requiring finer resolution, the offshore wave model had a nesting capability. This nesting allows for reducing the computational overhead of fine mesh calculations by utilizing a sequence of nested grids, each having a resolution finer than the preceding. The nested grids communicated through transfer of compatible boundary information. There was no limit to the number of nested grids that could be used during a WAVAD simulation.

A series of two nested grids was applied to the offshore wave simulation of the time period that spanned the deployment of the two acoustic Doppler current profilers. Grid #1 (Figure 2) was incremented in 0.25° (17.3 miles) squares and extended from 39.375° N to 44.625° N and 72.875° W to 63.125° W. There were 22 rows and 40 columns in grid #1. The maximum depth in Grid #1 was 4939 meters (16,205 feet). Grid #2 (Figure 3) was incremented in 0.05° (3.5 miles) squares and extended from 42.325° N to 44.675° N and from 71.175° W to 67.825° W. There were 48 rows and 68 columns in Grid #2. The maximum depth in Grid #2 was 290 meters (951.5 feet).

The WAVAD model required specification of bathymetry at each point in the computational grid. Water depths in Grid #1 and Grid #2 were found from the 30 arc second digital bathymetry constructed by the Coastal and Marine Geology Program of the United States Geological Survey (<http://woodshole.er.usgs.gov/project-pages/oracle/gomaine/bathy/>). The digital bathymetry was constructed using various data sources:

- NOAA Hydrographic Survey Data and NGDC Marine Trackline Geophysics Data
- Naval Oceanographic Office Digital Bathymetric Data Base - Variable Resolution gridded bathymetry
- Supplemental Datasets from Bedford Institute of Oceanography and Brookhaven National Laboratory
- NOAA Medium resolution digital Shoreline and DMA World Vector Shoreline
- Defense Mapping Agency ETOPO5 Digital relief of the Surface of the Earth
- GEBCO General Bathymetric Chart of the Oceans
- USGS North American 30 arc-second Digital Elevation Model (DEM)

The digital bathymetry contained both positive (land) and negative (sea floor) values in meters referenced to mean sea level. WAVAD required that all values be positive and in meters. All land values were converted to 0 and all ocean values were converted to positive values.

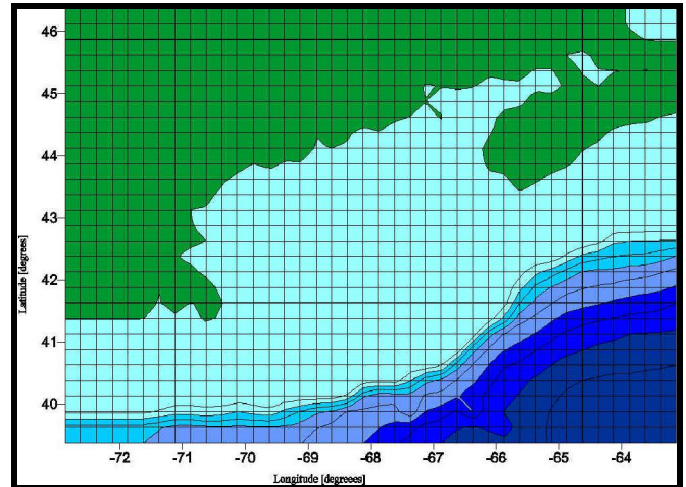


Figure 2. Grid #1 used in WAVAD model.

4.2. Options File

The options input file contained many of the parameters needed for the wave model. Along with the depth grid, a grid of the boundary conditions is located in this file. Some of the other parameters in the file include: the number of columns in the grid, number of rows in the grid, number of angle bands, number of frequency bands, distance between grid points, model time step, elevation of winds, number of hours between wind updates, options to read/write boundary data, option to write a variety of output files and latitude of lower left grid corner. In general, these parameters remained constant between the model runs; however, it was necessary to vary several parameters between the nested grid runs (i.e., numbers of columns, rows, latitude of lower left grid corner).

The WAVAD model was set such that the spectra were calculated across 72 degree bins and 29 frequency bins. The

frequencies investigated were 0.02 to 0.30 Hz at 0.01 Hz steps. These values were chosen based on the upper and lower limits of the deployed ADCPs. Wave height was solved as the first-moment of the one-dimensional energy spectrum.

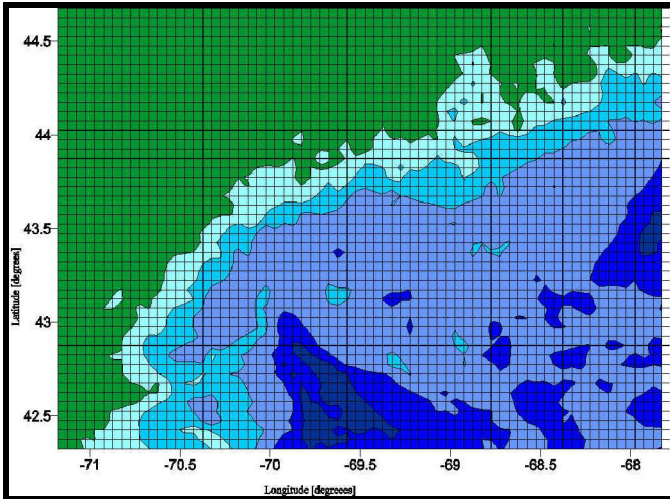


Figure 3. Grid #2 used in WAVAD model.

4.3. Wind Fields

Wind directions utilized by the model were in vector form. The vectors indicated the direction towards which the winds were blowing. Wind angles were referenced such that 0° was equal to 90° true N. The direction of rotation was counter-clockwise, therefore a wind angle of 180° was equal to 270° true N. Wind speeds were supplied to the model in the units of m/s and converted within the model to knots. The winds were assumed to be representative of a 10 m height above the water surface. For the Camp Ellis Beach study, wind fields were input every 12 hours. One input file containing the wind speeds and directions was used to model the deep-water waves.

The wind fields were created using the data from the National Aeronautics and Space Administration's QuikSCAT satellite. Aboard this satellite is a microwave scatterometer designed specifically to measure near-surface wind velocity (both speed and direction) over the global oceans under all weather conditions (SeaWinds). Scatterometers measure the wind indirectly. Atmospheric motions do not directly affect the radiation emitted by the scatterometer. The scatterometer transmits microwave pulses and receives backscattered power from the ocean surface. Changes in wind velocity and direction modify the ocean surface roughness, and are detectable through the backscattered power [4]. Since the satellite passes over the region twice during a 24 hour period, the time between wind field inputs was limited to 12 hours. For ease of use, it was assumed that the satellite passed over the region at 6 AM and 6 PM (GMT) everyday. These times were close to the actual time of passage. The wind fields were obtained from the Jet Propulsion Laboratory's Physical

Oceanography Distributed Active Archive Center (PO.DAAC). Both the ASCII data file and a colored image (Figure 4) were obtained.

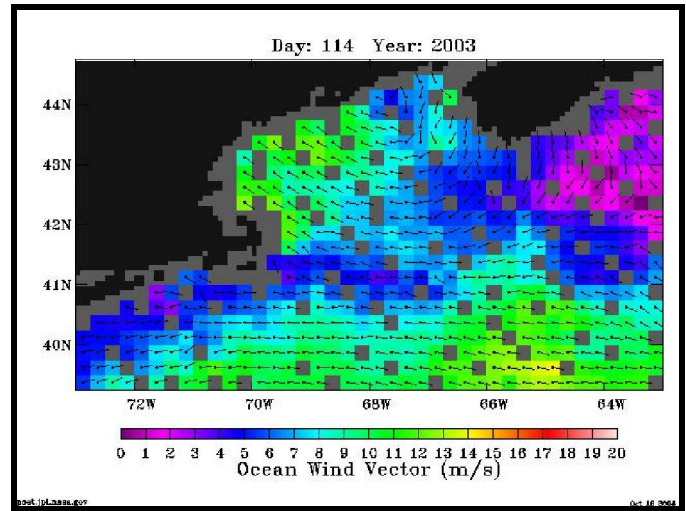


Figure 4. Example wind field from PO.DAAC.

Retrieval of the wind vectors near the shore using QuikSCAT imagery is impossible. The complex nature of waves in shallow water makes the retrieved vectors inaccurate. Since, the changes in ocean surface roughness near the coastline are not solely attributable to changes in wind. Several iterations were performed during the calibration process to make up for this deficiency. First, linear interpolation of the wind vectors along a row (constant latitude) was performed using the adjacent wind vectors to generate a mathematical equation to predict the wind vectors moving towards shore along that row. This process proved to over-predict the wave height as recorded by a nearshore National Oceanographic and Atmospheric Administration (NOAA) National Data Buoy Center (NDBC) buoy. The second iteration involved assuming that the wind speed goes to zero at the shore and therefore performed a linear interpolation between the last known wind vector and the shoreline along a row. This resulted in a decreasing wind speed as one traveled from offshore to onshore. The resultant WAVAD-calculated wave heights were too low at the nearshore buoy. The final approach involved utilizing the wind speeds recorded at the nearshore buoy and the winds recorded at Portland International Jetport, ME. The wind from the Jetport was assumed to be the wind at the shoreline, and linear interpolation was performed between the NOAA buoy and the shoreline. This methodology was used for all cases. The winds for the Jetport were retrieved digitally from the National Climatic Data Center. This method worked the best at predicting the nearshore buoy.

5. CALIBRATION AND VERIFICATION

Calibration and verification of the wave model required an ability to compare a time series of recorded wave heights from a nested wave gauge versus the calculated wave heights.

Since the purpose of using the generation scale model was to provide input for the nearshore wave model, the grid was never fine enough to compare with the deployed ADCP measured data. Instead, wave data in the Gulf of Maine were obtained from two NDBC buoys. These data consisted of hourly records of significant wave height, dominant wave period and a variety of meteorological measurements. The location of the two buoys can be found in Table 1.

The data used for comparison came from the results from Grid #2. Since the focus of the generation model was to provide adequate data for the transformation model, it was felt that calibrating to a wave record from a buoy lying only within the extent of Grid #1 but outside Grid #2 would not provide the desired results later in the modeling process. The two chosen buoys, 44005 and 44007, lie within both of the grids.

TABLE 1
LOCATION OF NDBC BUOYS

Buoy Number	Latitude [degrees N]	Longitude [degrees W]	Water Depth [m]
44007	43.53	70.14	18.9
44005	43.18	69.18	21.9

Previous use of the WAVAD model by Woods Hole Group [15] used a calibration method through modification of the wind speed. This is achieved within the computer model by using a multiplication factor that increased the wind speed. Calibration was achieved by matching the maximum wave height. The entire wind field was modified by this factor. The previous use of WAVAD was to determine the hurricane wave forces on a seawall. It was found during the 1991 project that a factor of 1.05 provided adequate calibration.

Initial tests for the wind factor for this Section 111 study ranged from 1.05 to 1.20 increase in wind speed. Evaluation of the maximum predicted and recorded wave height showed that the 1.05 case did a good job of predicting the maximum wave height. However, the results depicted that the modeled wave did not decay at the same rate as the measured wave.

The wave decay issue was addressed in three ways. The first method was to add an additional numerical grid to the front of the WAVAD model run. This grid was incremented on 1° squares and extended from 35° N to 45° N and 75° W to 60° W. Results from this set of model runs did not increase the accuracy of the model. Based on the governing equations, which are of a form similar to those used for wind wave growth in the USACE Coastal Engineering Manual [14], as shown below, the wind fields were artificially increased to determine if wind magnitude had a potential influence on the decay mechanism.

$$\frac{gH_{m_0}}{u_*^2} = 4.13 * 10^{-2} * \left(\frac{gX}{u_*^2} \right)^{\frac{1}{2}}$$

and

$$\frac{gT_p}{u_*} = 2.727 \left(\frac{gX}{u_*^2} \right)^{\frac{1}{3}}$$

Where u_* is the wind friction velocity and X is the fetch distance. A third method is currently being investigated is modification of the bottom friction factor based on newer reported friction coefficients.

The modeled wave heights were compared to the measured wave heights at both of the buoy locations. Although the offshore modeling goal is to pass on a wave spectrum as input into STWAVE, validity of the WAVAD output was based upon matching the maximum modeled wave height. Matching the maximum wave height would ensure that the proper amount of energy was being directed into the spectrum being used as input into the wave transformation model.

5.1. Calibration

The WAVAD model was calibrated using data recorded during the time period April 24-28, 2003. This time period was within the deployment of the two ADCPs. Both ADCPs recorded a wave event during this time period greater than 1 m in height. This time period also corresponded with good return from the QuikSCAT satellite. Using the previously described methodology, WAVAD was executed and compared.

Figure 5 compares the measured and calculated wave heights at buoy 44005. WAVAD took some time to spin up, but it was capable of modeling the small peak in wave height recorded midday on 4/26. It over-predicted this small event, but its ability to get this small feature with the 12-hour spaced wind field input is remarkable. The relative error between maximum recorded and modeled wave heights was 5.7%.

Results from the nearshore buoy did not show as good of results (Figure 6). The model once again showed that small increase in wave height within the storm growth midday of the 26th. However, the overall ability of WAVAD to model the maximum wave height as recorded by the storm was not as good as Buoy 44005. The error between modeled and measured wave height was 13.9%. It was felt that the error difference between the two buoy locations was either indicative of the lack of wind data in the nearshore zone or of more complex physical processes outside of the capabilities of WAVAD.

The WAVAD model computed variations in energy density throughout the duration of the calibration time period. High energy densities correspond with large waves and low energy densities correspond with smaller waves. Therefore, energy density is a measure of storm intensity. Groupings of energy density in more than one frequency band indicate the

presence of two or more wave trains having different wave periods. Groupings of energy density at isolated times during the storm indicate the presence of two or more peaks in storm intensity, or the passage of multiple fronts.

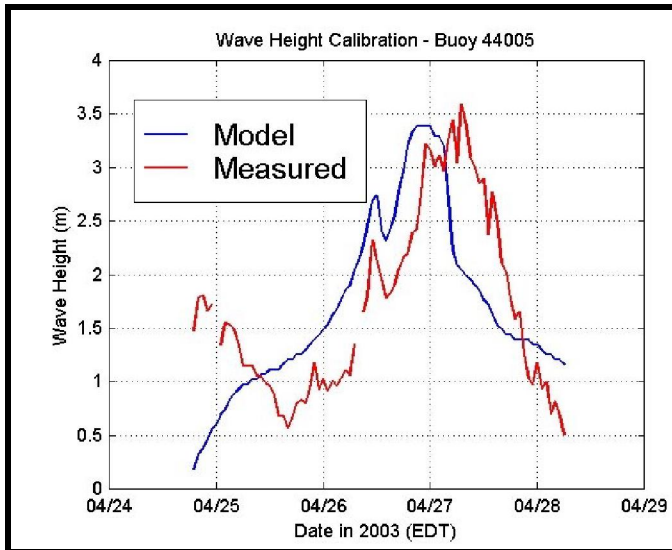


Figure 5. Comparison of modeled and measured wave heights at NOAA Buoy 44005 during calibration time period.

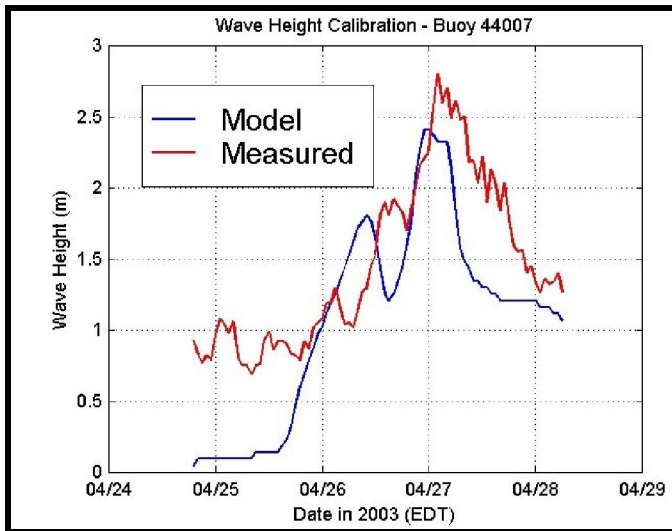


Figure 6. Comparison of modeled and measured wave heights at NOAA Buoy 44007 during calibration time period.

Figure 7 represents a contour plot of the one-dimensional energy spectra during the calibration time period at NOAA Buoy 44007. The groupings of energy early on the 26th and once again on the 27th indicate the presence of either two fronts or two peaks in storm intensity during the time period. This feature is also present in the wave height comparison plots. Figure 7 also shows energy spreading into the lower frequencies as the storm continues.

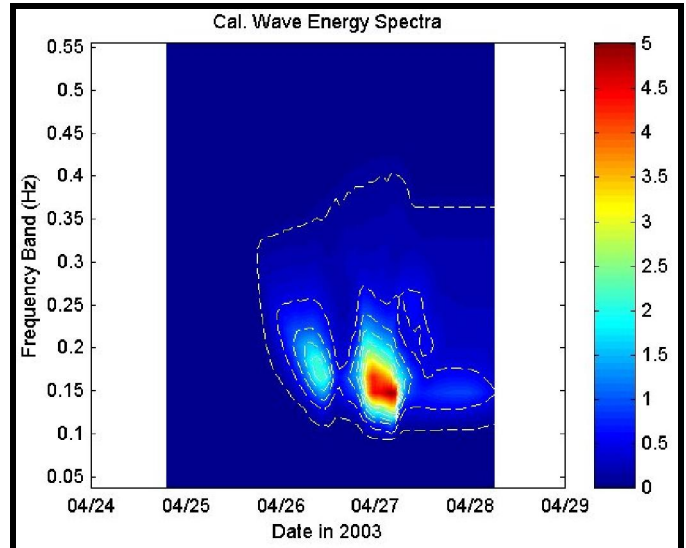


Figure 7. Contour plot of one-dimensional energy spectra during calibration time period at NOAA Buoy 44007.

5.2. Verification

To verify that the method used to calibrate WAVAD was valid, a second time period was chosen for verification. Once again, a time period that had a relatively large wave event corresponding to the deployment of the ADCPs and sufficient QuikSCAT data was used. This time period was April 01-07, 2003.

Figure 8 compares the measured and modeled wave heights at Buoy 44005. WAVAD once again depicts the peak during the storm growth and decays at almost the same rate as the measured data. The relative error between maximum wave heights was 5.3%, which is about the same as the error during the calibration case. The results from Buoy 44007 (Figure 9) once again are not as good as those from Buoy 44005. The error between measured and model wave heights is 16.8%, which is comparable to the result seen in calibration.

A contour plot of the one-dimensional energy spectra during the verification time period at NOAA Buoy 44007 (Figure 10) indicates the presence of three potential fronts or peaks in storm intensity. Also, more energy is leaked into the lower frequencies and the maximum energy density occurs over a short time period.

6. CONCLUSIONS

Because of the lack of temporal and spatial similitude between locally observed wave information and available data sources, a generation-scale wave model was used to develop input into the detailed, shallow-water transformation-scale wave model. These two models were part of an extensive wave modeling system used to analyze the potential impacts of structural modifications to a federally constructed and maintained navigational structure in Saco, ME. The

generation-scale numerical model was calibrated and verified using satellite observed wind fields and local point measurements as source data. The calibration between the measured and modeled maximum wave height varied between 5 and 17%. These errors are acceptable when looking at the bigger picture of the overall success of the initial goal of supplying input into the transformation-scale model. The transformation scale model had a bias of -0.02 m and an RMS error of 0.11m at the offshore ADCP location while the nearshore ADCP had bias of -0.21 m and an RMS error of 0.23m. These low RMS errors show that using WAVAD as a potential spectral wave data source for detailed, shallow-water transformation-scale models can help engineers fill in temporal and spatial gaps.

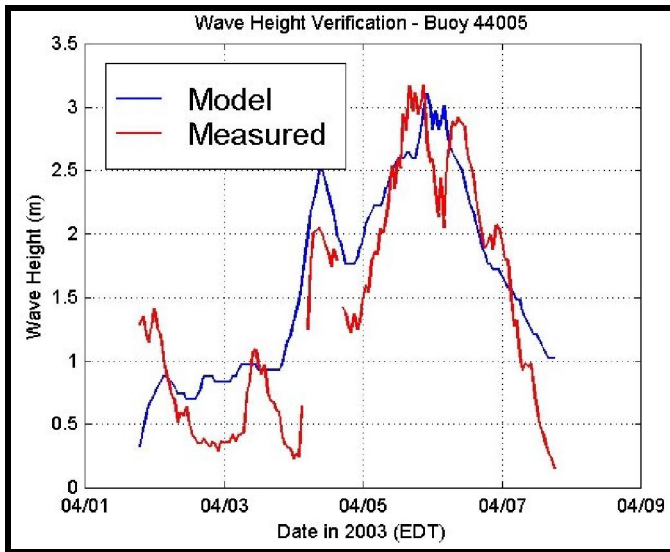


Figure 8. Comparison of modeled and measured wave heights at NOAA Buoy 44005 during verification time period.

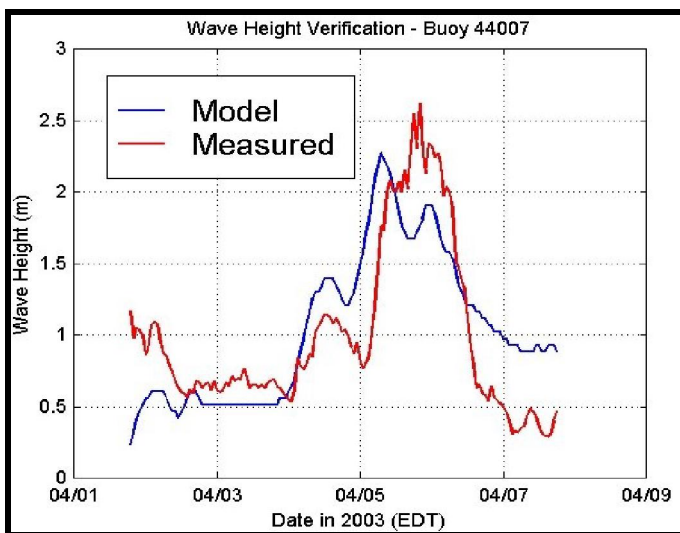


Figure 9. Comparison of modeled and measured wave heights at NOAA Buoy 44007 during verification time period.

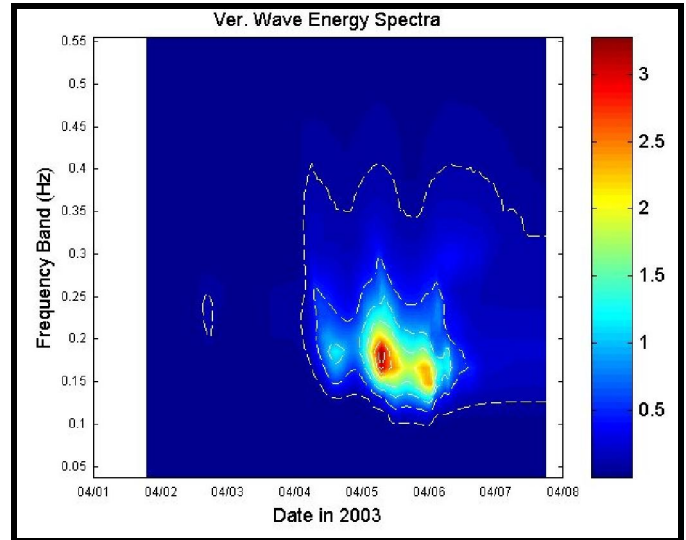


Figure 10. Energy spectra during verification time period.

7. ACKNOWLEDGMENT

The authors wish to thank the US Army Corps of Engineers, New England District and the Maine Geological Survey for their support with the program. David Aubrey provided a review of the manuscript. This is Woods Hole Group Publication 2004-010.

8. REFERENCES

- [1] Bosma, K. and B. Caufield, "Integration of Multiple Wave Models from Generation Scale to Nearshore Scale. A Practical Application in Maine, USA," 8th International Wave Hindcasting and Forecasting Workshop, Oahu, Hawaii, 2004.
- [2] Collins, J., "Prediction of Shallow-Water Spectra," *Journal of Geophysical Research*, Vol. 77, p. 2693-2707, 1972.
- [3] Forristall, G., "Measurements of a Saturated Range in Ocean Wave Spectra," *Journal of Geophysical Research*, Vol. 86, p. 8075-8094, 1981
- [4] Jet Propulsion Laboratory, SeaWinds Science Data Product: User's Manual. Ed. Ted Lungu, California Institute of Technology, 2002.
- [5] Kahma, K., "A Study of the Growth of the New Wave Spectrum with Fetch," *Journal of Physical Oceanography*, Vol. 11, p. 1503-1515, 1981.
- [6] Kitaigorodskii, S., "On the Theory of the Equilibrium Range in the Spectrum of Wind-Generated Gravity Waves," *Journal of Physical Oceanography*, Vol. 13, p. 816-827, 1983.
- [7] Maine State Planning Office, Improving Maine's Beaches: Recommendations of the Southern Maine Beach Stakeholder Group, Maine State Planning Office, Augusta, Maine, 1998.
- [8] Resio, D., "The Estimation of Wind-Wave Generation in a Discrete Model," *Journal of Physical Oceanography*, Vol. 11, p. 510-525, 1981.
- [9] Resio, D., "Shallow-Water Waves-Part I: Theory," *Journal of Waterway, Port, Coastal and Ocean Engineering*, Vol. 113, p 266-283, 1987.

- [10] Resio, D., "Shallow-Water Waves-Part II: Data Comparison," *Journal of Waterway, Port, Coastal and Ocean Engineering*, Vol. 114, p. 50-65, 1988.
- [11] Resio, D., Program WAVAD: Global/Regional Wave Model for Wave Prediction in Deep and/or Shallow Water. Offshore & Coastal Technologies, Inc., 1990.
- [12] Slovinsky, Peter A. and Dickson, Stephen M., Variation of Beach Morphology Along the Saco Bay Littoral Cell An Analysis of Recent Trends and Management Alternatives, Maine Geol. Survey, Open-file Report 03-78, 2003.
- [13] Toba, Y., "Stochastic Form of the Growth of Wind Waves in a Single-Parameter representations with Physical Implications," *Journal of Physical Oceanography*, Vol. 8, p. 494-507, 1978.
- [14] United State Army Corps of Engineers, Coastal Engineering Manual, Part II, Chapter 1. Water Wave Mechanics, Ed. Z. Demirbilek and C.L. Vincent, 1996.
- [15] Woods Hole Group (formerly Aubrey Consulting, Inc.), "Deer Island Extremal Wave Analysis and Physical Modeling: Final Report," 1991.